

# Soil-Water Partitioning Behavior of Oxyfluorfen Under California Rice Field Conditions

David J. Bonnar,\* Jeff P. Eichler, Sanjai J. Parikh, Andrew Blandino, Rebecca A. Lybrand, Madison L. Morris, Matt J. Hengel, and Ronald S. Tjeerdema

Cite This: <https://doi.org/10.1021/acsagstech.3c00341>

Read Online

ACCESS |

Metrics & More

Article Recommendations

Supporting Information

**ABSTRACT:** The herbicide oxyfluorfen [OXY; 2-chloro-1-(3-ethoxy-4-nitrophenoxy)-4-(trifluoromethyl)benzene] has recently surged in interest among rice farmers with the development of OXY-tolerant rice and its demonstrated effectiveness against problematic rice weeds in California. Not currently registered for use with rice, its fate in rice fields is poorly understood. Using a batch equilibrium method, we characterize the soil-water partitioning behavior of OXY under simulated California rice field conditions. Sorption data imply strong, primarily concentration-independent binding correlated with soil organic carbon ( $\log[K_{oc}]$  4.79–5.19;  $N$  0.87–1.08) across all soil, temperature, and salinity treatments. Temperature significantly enhanced binding affinity for sorption and desorption processes ( $P < 0.01$ ). Bound OXY was poorly desorbed (9.3 to 27.0% desorption) from rice soils and exhibited significant sorption hysteresis ( $HI > 0$ ) in all treatments. These results indicate that OXY will predominantly remain in soil and will be resistant to release into water in California rice fields.

**KEYWORDS:** herbicide, weedy rice, sorption, desorption, isotherm, hysteresis

## INTRODUCTION

Oxyfluorfen (OXY, trade name Goal, [Figure 1](#)) is a broad-spectrum, diphenyl-ether herbicide used for pre- and

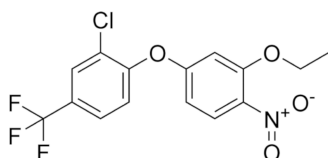


**Figure 1.** Structure of oxyfluorfen.

postemergent control of broadleaf and grassy weeds.<sup>1</sup> First registered in 1979, OXY has seen wide use in both agricultural and nonagricultural settings, with the majority of agricultural usage occurring within California.<sup>2</sup>

Despite entering the market over 40 years ago, interest in its use in California rice fields has piqued recently due in part to technological advancements such as the development of nontransgenic, OXY-tolerant rice strains and research indicating effective control of rice weeds.<sup>3,4</sup> Of particular interest to growers, OXY has been shown to be effective against the rice weed *Oryza sativa f. spontanea* (weedy rice), a pest for which no herbicides are currently registered in California.<sup>4</sup> Although there are currently no OXY products registered for use in rice fields, efforts are underway to bring them to market.<sup>3,4</sup> Use in rice fields represents a new use pattern for OXY as all currently registered products in the U.S. contain general and explicit prohibitions against applications in- or near-aquatic resources due in part to its high toxicity to aquatic organisms.<sup>1,2</sup> Despite the use restrictions, OXY has been frequently detected in sediment and surface water, and use within rice fields enhances

the potential for release into adjacent waters.<sup>5,6</sup> Thus, the fate of OXY under California rice field conditions must be well understood to inform effective and environmentally protective use practices.

Most rice produced in California is grown within the Sacramento Valley, where growers flood fields before planting and maintain water levels at approximately 10 cm throughout the growing season.<sup>4,7</sup> These waters often experience seasonal temperature variations, with observed fluctuations ranging from 5 to 38 °C.<sup>8,9</sup> At higher temperatures, evapoconcentration can increase field salinity, with levels reaching up to 6.0 dS·m<sup>-1</sup> in some California fields.<sup>10</sup> As 0.88 dS·m<sup>-1</sup> is the salinity threshold for crop yield reduction, growers are vested in ensuring field water is not held for too long.<sup>10,11</sup> However, when herbicides are applied, water holding periods are regularly imposed, limiting how early water can be released from fields to allow herbicides to dissipate.<sup>12</sup> The period for an herbicide to dissipate below levels of concern is chemically specific and depends on its properties and fate.

One of the most influential processes governing herbicide fate is soil-water partitioning.<sup>13</sup> Frequently characterized by the partition coefficient  $K_d$ , it is the primary chemodynamic process responsible for how much herbicide is found in soil versus water. Measurement of  $K_d$  is impacted by temperature and salinity levels, which influence aqueous solubility and

**Received:** September 1, 2023

**Revised:** October 20, 2023

**Accepted:** November 3, 2023

Table 1. Rice Field Soil Properties<sup>a</sup>

soil	texture <sup>b</sup>	sand (%)	silt (%)	clay (%)	$f_{om}$	$f_{oc}$	pH	CEC (meq/100 g)
Davis	clay loam	22	43	35	0.0415	0.0241	6.42	37.3
Biggs	clay loam	33	40	27	0.0277	0.0161	5.37	20.2

<sup>a</sup>Abbreviations: fraction organic matter ( $f_{om}$ ), fraction organic carbon ( $f_{oc}$ ), cation exchange capacity (CEC). <sup>b</sup>Texture defined according to Natural Resources Conservation Service soil texture classification.

sorption to sediment.<sup>14,15</sup> Soils rich in organic matter and clay content, such as rice fields, are known to strongly bind nonpolar, hydrophobic chemicals such as OXY, and bound herbicides may not be readily desorbed.<sup>16,17</sup>

Although rice fields are unique agricultural environments that vary considerably in environmental conditions pertinent to chemical fate, the soil-water partitioning of OXY has not been characterized in California rice fields. Thus, this study's overarching objective is to investigate the soil-water partitioning behavior of OXY under simulated California rice field conditions. Specifically, (1) the batch equilibrium method is used to evaluate OXY sorption and determine  $K_d$  and the organic carbon-water partitioning coefficient ( $K_{oc}$ ) in two California rice field soils under simulated California conditions (e.g., temperature, salinity); (2) the organic matter characteristics and mineralogy of the soils are profiled; and (3) desorption processes are characterized to evaluate sorption reversibility.

## MATERIALS AND METHODS

**Chemicals.** 2-Chloro-1-(3-ethoxy-4-nitrophenoxy)-4-(trifluoromethyl)benzene (OXY; 98%) was purchased from Ontario Chemicals, Inc. (Guelph, ON). Water (Optima grade), methanol (Optima grade), acetonitrile (HPLC grade), sodium chloride (99%), and calcium chloride (100%) were purchased from Fisher Scientific (Fair Lawn, NJ). Formic acid (98%) was purchased from Honeywell International, Inc. (Muskegon, MI). Water (HPLC grade), ethyl acetate (HPLC grade), 2-chloro-1-(3-ethoxy-d6-4-nitrophenoxy)-4-(trifluoromethyl)benzene (d5-OXY; 98%), magnesium sulfate, and sodium sulfate were purchased from Sigma-Aldrich (St. Louis, MO).

**Soil Preparation and Analysis.** Soils were collected from two separate rice fields near Davis, CA (38.543936, -121.650750; Riz-Sycamore clay loam), and in Biggs, CA (39.451826, -121.719226; Esquon-Neerdohe fine, smectic, flood basin soil).<sup>18,19</sup> They were collected from the top 10 cm of each field, air-dried, and sieved (<2 mm) for use in partitioning experiments. Soil properties, including texture, fractions of organic matter ( $f_{om}$ ), fraction of organic carbon ( $f_{oc}$ ), and cation exchange capacity (CEC), were characterized by the UC Davis Analytical Laboratory, while soil pH was measured according to methods described by U.S. Salinity Laboratory Staff.<sup>20,21</sup> A summary of these properties is presented in Table 1.

Soil organic matter (SOM) content and soil mineralogy were qualitatively analyzed using Fourier transform infrared (FTIR) spectroscopy and X-ray diffraction (XRD), respectively. Methodologies for these analyses are presented in the Supporting Information.

**Soil-Water Partitioning.** Sorption and desorption isotherms were constructed according to OECD 106 batch equilibrium method guidelines.<sup>22</sup> The optimal soil-to-solution ratio of 1:600 (0.25 g of soil and 150 g of 0.01 M CaCl<sub>2</sub> water) was determined during preliminary studies and selected for all isotherms. Additional preliminary studies also showed sorption and desorption pseudoequilibrium durations of 48 and 24 h, respectively, and that OXY was stable to degradation (e.g., hydrolysis and biotic) throughout the experiment. Soil-water samples were prepared in 150 mL crimp-top glass serum bottles and equilibrated overnight in a MaxQ 6000 temperature-controlled shaker (265 rpm; Thermo Scientific, Waltham, MA). Samples were then spiked to initial concentrations of 0.009, 0.015, 0.03, 0.05, or 0.09  $\mu\text{g}\cdot\text{g}^{-1}$  OXY in the aqueous phase (acetonitrile concentration did not

exceed 0.1%). Three replicates for each spike level and a negative control were prepared for each experiment. Spiked samples were shaken (265 rpm) for 48 h prior to centrifugation (1573g, 15 min) and liquid-liquid extraction of aqueous phase aliquots (described below). The remaining aqueous phase was then decanted and replaced with 150 g of fresh 0.01 M CaCl<sub>2</sub> aqueous solution to prepare samples for desorption analysis. Desorption samples were shaken (265 rpm) for 24 h before centrifugation (1573g, 15 min) and liquid-liquid extraction of the aqueous phase under the same conditions as the sorption analysis. The experiment was repeated for both soils at equilibration temperatures of 15, 25, and 35 °C ( $\pm 1$  °C). An additional set of isotherms at 25 °C ( $\pm 1$  °C) were prepared under the same conditions as before, except with an aqueous phase mixture of either 0.01 or 0.05 M NaCl, CaCl<sub>2</sub>, MgSO<sub>4</sub>, and Na<sub>2</sub>SO<sub>4</sub> at a 10:1:2:1 molar ratio. These salinity levels (approximately 1.2 and 6.0 dS·m<sup>-1</sup>) and salt composition were selected to simulate observed California rice field salinity (RFS) conditions.<sup>10,11</sup>

**Aqueous Phase Extraction.** Five (5) mL of aqueous phase was transferred to 15 mL polypropylene centrifuge tubes, followed by 5 mL of ethyl acetate. Tubes were capped and shaken vigorously by hand for 2 min. The samples were allowed to settle before transferring 3.5 mL of the organic layer to borosilicate test vials and evaporating to dryness under gentle N<sub>2</sub> flow in a water bath (50 °C). Samples were reconstituted with 3.5 mL of acetonitrile containing 0.01  $\mu\text{g}\cdot\text{mL}^{-1}$  d5-OXY internal standard, vortexed, then filtered (0.2  $\mu\text{m}$ , PTFE) into sample vials for liquid chromatography-tandem mass spectrometry analysis. Preliminary investigations indicated no loss of OXY due to filtration. Spike recovery was evaluated in control bottles containing a spiked aqueous phase. Average spike recovery ( $\pm$ SE) at a fortification level of 0.015  $\mu\text{g}\cdot\text{g}^{-1}$  was  $95 \pm 1.8\%$  ( $n = 3$ ). Sorption of analyte to container walls was determined to be a source of loss in these control samples, with extractable residues typically less than 0.5% and not exceeding 1.12% of the applied amount. Correction for container sorption, however, was deemed unnecessary as the presence of soil is known to mitigate this loss, and no extractable residues were detected on container walls in preliminary studies of samples containing soil.<sup>22</sup>

**LC-MS/MS Analysis.** Sample extracts were analyzed with an Agilent 1260 Infinity series high-pressure liquid chromatograph (HPLC) (Santa Clara, CA) in tandem with an Agilent 6420 triple quadrupole mass spectrometer (QQQ) using electrospray ionization in positive mode. Sample injections (10  $\mu\text{L}$ ) were made onto an Agilent ZORBAX Eclipse XDB-C18 column (4.6 mm  $\times$  150 mm; 5  $\mu\text{m}$ ) and eluted with isocratic mobile phase composed of 90% methanol (0.1% formic acid) and 10% water (0.1% formic acid) at 0.5 mL·min<sup>-1</sup>. A deuterated isotope of oxyfluorfen, d5-OXY, was included as an internal standard to account for instrumental variation, as matrix effects were not observed in preliminary studies. Retention times for both OXY and d5-OXY were 5.6 min, with a stop-time of 8 min. Mass analysis was performed using multiple transition monitoring. Selected quantitative and qualitative ions for OXY were 362  $\rightarrow$  316 and 362  $\rightarrow$  237, and 367  $\rightarrow$  237 m·z<sup>-1</sup> for d5-OXY. Linear calibration curves were constructed over five concentrations between 0.0005 and 0.5  $\mu\text{g}\cdot\text{mL}^{-1}$  oxyfluorfen in acetonitrile ( $R^2$  0.996–0.999). Additional mass spectrometer acquisition parameters are available in the Supporting Information (Table S1).

Method detection limits (MDL) and method quantitation limits (MQL) were determined by analyzing blank extracts ( $n = 7$ ) spiked to 0.001  $\mu\text{g}\cdot\text{mL}^{-1}$  of OXY in acetonitrile. The MDL and MQL were calculated by multiplying the standard deviation of the replicate spiked blanks by 3.1427 (single-tailed 99th percentile t-statistic) and 10, respectively. For Davis soil treatments, the MDL and MQL were

0.00031 and 0.00099  $\mu\text{g}\cdot\text{mL}^{-1}$ , respectively. For Biggs soil treatments, the MDL and MQL were 0.00006 and 0.00019  $\mu\text{g}\cdot\text{mL}^{-1}$ , respectively.

**Partitioning Coefficients.** The concentration of the aqueous phase after equilibration was determined directly from aqueous phase extracts. Consistent with method standards outlined by OECD 106 guidelines, concentration in soil at equilibrium was calculated via the measure by difference method.<sup>13,22</sup> For all calculations, soil mass refers to oven dry mass, which is the weight of soil corrected for moisture content.

The concentration in the soil at sorption equilibrium was calculated according to eq 1:

$$q_s^s = \frac{m_{\text{aq}} \cdot (C_i - C_{\text{aq}}^s)}{m_s} \quad (1)$$

where  $m_{\text{aq}}$  and  $m_s$  are the mass (g) of the aqueous phase and soil, respectively,  $C_i$  is the initial aqueous concentration of OXY ( $\mu\text{g}\cdot\text{g}^{-1}$ ), and  $q_s^s$  and  $C_{\text{aq}}^s$  are the concentration of OXY ( $\mu\text{g}\cdot\text{g}^{-1}$ ) in soil and aqueous phase at sorption equilibrium, respectively.

The concentration in the soil at desorption equilibrium was calculated according to eq 2:

$$q_s^d = \frac{C_i \cdot m_{\text{aq}}^i - (C_{\text{aq}}^s \cdot m_{\text{aq}}^{\text{dec}} + C_{\text{aq}}^d \cdot m_{\text{aq}}^r)}{m_s} \quad (2)$$

where  $m_{\text{aq}}^i$  is the initial aqueous phase mass (g),  $m_{\text{aq}}^{\text{dec}}$  is the mass of aqueous phase decanted (g),  $m_{\text{aq}}^r$  is the mass of aqueous phase after replacing the mass of the decanted liquid (g), and  $q_s^d$  and  $C_{\text{aq}}^d$  are the concentration of OXY ( $\mu\text{g}\cdot\text{g}^{-1}$ ) in soil and aqueous phase at desorption equilibrium, respectively.

The soil-water partition coefficient ( $K_d$ ) and organic carbon-water partition coefficient ( $K_{\text{oc}}$ ) were calculated from data obtained from the second lowest initial concentration ( $C_i = 0.015 \mu\text{g}\cdot\text{g}^{-1}$ ) according to eqs 3 and 4:

$$K_d = \frac{q_s^s}{C_{\text{aq}}^s} \quad (3)$$

$$K_{\text{oc}} = \frac{K_d}{f_{\text{oc}}} \quad (4)$$

where  $f_{\text{oc}}$  is the fraction of organic carbon of the soil (Table 1).

**Freundlich Isotherms.** Sorption and desorption isotherms were constructed by plotting the equilibrium concentration in soil,  $q_s$ , versus the equilibrium concentration in water,  $C_{\text{aq}}$ , for the various treatment groups. Isotherms were then fit to the log transformed Freundlich eq 5:

$$\log(q_s) = N \cdot \log(C_{\text{aq}}) + \log(K_F) \quad (5)$$

where  $q_s$  and  $C_{\text{aq}}$  are the equilibrium concentration OXY sorbed to the soil and water ( $\mu\text{g}\cdot\text{g}^{-1}$ ), respectively,  $N$  is the Freundlich exponent, and  $K_F$  is the Freundlich constant.

**Hysteresis.** The degree of sorption–desorption hysteresis was quantified through calculation of the hysteresis index (HI) according to eq 6:

$$\text{HI} = \frac{q_e^d - q_e^s}{q_e^s} \quad (6)$$

where  $q_e^d$  and  $q_e^s$  are the solid-phase solute concentrations for a single-cycle sorption and desorption experiment, respectively, and are calculated at a particular residual solution phase concentration ( $C_e$ ) using the Freundlich parameters.<sup>23</sup> A zero or negative HI value indicates that hysteresis is insignificant, while values greater than 0 indicate increasing degrees of sorption–desorption hysteresis.<sup>24</sup> Lower and upper bound  $C_e$  for calculation of HI were selected based on the observed sorption and desorption isotherm ranges for each treatment.

**Statistics.** The effect of soil, temperature, and saline environment on Freundlich parameters of eq 5 was assessed using a weighted linear

regression model with separate  $N$  and  $\log(K_F)$ , slope, and intercept, respectively, for each experimental treatment combination of soil, temperature, and saline environment for both sorption and desorption processes. The same model was used to calculate HI of eq 6 as a transformation of eq 5 for both sorption and desorption isotherms and for each treatment combination.

Due to the presence of measurement error for both  $C_{\text{aq}}$  and  $q_s$  at each  $C_i$ , which can bias model estimates of Freundlich parameters, the regression model was fit on the average of three replicate values for  $q_s$  and  $C_{\text{aq}}$  at each  $C_i$  and for each treatment combination in order to reduce such bias. Exploratory analysis demonstrated heteroskedasticity of model residuals across different treatments with standard linear regression, and as a result, weighted linear regression was considered instead.

Data were analyzed using R statistical software (Vienna, Austria) using the **nlme** R package with the `gls()` function for weighted least-squares.<sup>25,26</sup> A significance level ( $\alpha$ ) of 0.05 was selected, and results where  $P \leq 0.05$  were considered statistically significant.

## RESULTS AND DISCUSSION

**Soil Organic Matter and Mineralogy.** Figure S1 in the Supporting Information provides FTIR spectra to compare the mineral and SOM compositions of the Davis and Biggs soils. Few differences can be observed in the spectra of the unaltered soil samples (spectra c and d), which include both mineral and SOM fractions; however, examining the SOM spectra (spectra a and b) reveals notable differences between the two soils.

Both samples show IR peaks consistent with those attributed to aromatic carbon ( $1552 \text{ cm}^{-1}$ ) and carboxylic acids ( $1548$  and  $1425 \text{ cm}^{-1}$ ). The primary difference between the SOM spectra is that the organic peak intensities are greater for the Davis soil than the Biggs soil, which is consistent with the  $f_{\text{oc}}$  values reported in Table 1. The peak at  $1710 \text{ cm}^{-1}$  in spectrum b represents carbonyl (C=O) due to the protonation of carboxyl groups—which is explained by the lower pH of the Biggs soil (Table 1). The general carbon chemistry appears similar for the two soils, which is further demonstrated via examination of the relative ratio of the aromatic peak ( $1552 \text{ cm}^{-1}$ ) to the carboxyl peaks ( $1548$  and  $1425 \text{ cm}^{-1}$ ) of the OM spectra: Davis  $1552:1548 = 1.14$ , Davis  $1552:1425 = 1.18$ , Biggs  $1552:1548 = 1.18$ , and Biggs  $1552:1425 = 1.13$ .

Figure S2 in the Supporting Information provides X-ray diffractogram patterns for mineralogical characterization. The primary mineral compositions for the Biggs and Davis surface soils were relatively similar in that both samples were dominated by quartz and plagioclase feldspar minerals, with more minor amounts of mica and secondary clays (Figure S2). The primary mineral assemblage for the Biggs soil was dominated by quartz and feldspars (i.e., labradorite and albite; Figure S2a), which was comparable to the Davis soil that was also predominately quartz and feldspar minerals (i.e., albite and oligoclase; Figure S2b). The  $9.95 \text{ \AA}$  peak indicative of mica (i.e., phlogopite) was most pronounced in the Davis sample versus a much lower intensity peak expression in the Biggs sample. Peaks observed in the lower d-spacing range of the bulk Davis sample also suggested the presence of vermiculite ( $14.1 \text{ \AA}$ ), illite ( $10.1 \text{ \AA}$ ), and kaolinite ( $7.2 \text{ \AA}$ ). The diffractogram for the Biggs soil confirmed the presence of kaolinite, vermiculite, and illite as well as an interlayered mineral that was distinguished by partial collapse following the KCl-550 heat treatment (Figure S2c). There was also little to no smectite present in the Biggs soil compared to a well-expressed peak at  $18.4 \text{ \AA}$  indicative of smectite in the Davis soil following Mg + Glycerol treatment. The clay mineral

**Table 2. Freundlich Parameters for Sorption of OXY in California Rice Field Soils<sup>a,b</sup>**

soil	temperature (°C)	salinity (M)	log( $K_{oc}$ ) <sup>c</sup> ± SE	$N$ ± SE	log( $K_F$ ) ± SE	$R^2$
Davis	15	0.01 CaCl <sub>2</sub>	4.79 ± 0.02 a	1.08 ± 0.10 ab	3.36 ± 0.22 a	0.984
	25	0.01 CaCl <sub>2</sub>	4.82 ± 0.04 ab	0.92 ± 0.02 <sup>d</sup> ab	3.02 ± 0.05 a	0.998
	35	0.01 CaCl <sub>2</sub>	5.00 ± 0.01 ab	1.00 ± 0.11ab	3.44 ± 0.26 a	0.978
	25	0.01 RFS	4.82 ± 0.04 ab	0.99 ± 0.08 ab	3.19 ± 0.16 a	0.973
	25	0.05 RFS	4.87 ± 0.04 ab	0.88 ± 0.09 ab	2.92 ± 0.18 a	0.988
Biggs	15	0.01 CaCl <sub>2</sub>	4.88 ± 0.03 b	1.01 ± 0.14 ab	3.13 ± 0.29 a	0.971
	25	0.01 CaCl <sub>2</sub>	5.07 ± 0.01 ab	0.99 ± 0.08 ab	3.17 ± 0.16 a	0.977
	35	0.01 CaCl <sub>2</sub>	5.19 ± 0.07 ab	0.87 ± 0.02 <sup>d</sup> b	3.05 ± 0.04 a	0.998
	25	0.01 RFS	4.86 ± 0.06 ab	1.05 ± 0.04 a	3.20 ± 0.09 a	0.994
	25	0.05 RFS	4.83 ± 0.02 ab	1.01 ± 0.02 a	3.08 ± 0.05 a	0.998

<sup>a</sup>Letters indicate statistically significant differences between treatments. Values with the same letter are not significantly different, while those with different letters are statistically distinct ( $\alpha = 0.05$ ). <sup>b</sup>Abbreviations: oxyfluorfen (OXY), rice field salinity (RFS) with a molar ratio of 10:1:2:1 NaCl:CaCl<sub>2</sub>:MgSO<sub>4</sub>:Na<sub>2</sub>SO<sub>4</sub>. <sup>c</sup>Calculated from data obtained when initial concentration ( $C_i$ ) is 0.015  $\mu\text{g}\cdot\text{g}^{-1}$ . <sup>d</sup>Freundlich slope ( $N$ ) significantly different ( $P < 0.05$ ) from 1.

**Table 3. Freundlich Parameters for Desorption of OXY in California Rice Field Soils<sup>a,b</sup>**

soil	temperature (°C)	salinity (M)	log( $K_{oc}$ ) <sup>c</sup> ± SE	$N$ ± SE	log( $K_F$ ) ± SE	$R^2$
Davis	15	0.01 CaCl <sub>2</sub>	5.10 ± 0.02 a	0.99 ± 0.03 a	3.47 ± 0.08 a	0.998
	25	0.01 CaCl <sub>2</sub>	5.15 ± 0.06 abc	0.94 ± 0.03 ab	3.36 ± 0.07 <sup>d</sup> a	0.997
	35	0.01 CaCl <sub>2</sub>	5.34 ± 0.02 bc	0.91 ± 0.04 abc	3.43 ± 0.10 a	0.997
	25	0.01 RFS	5.15 ± 0.02 ac	1.11 ± 0.01 abc	3.83 ± 0.25 <sup>d</sup> a	0.963
	25	0.05 RFS	5.07 ± 0.02 a	0.83 ± 0.07 abc	3.03 ± 0.16 ab	0.992
Biggs	15	0.01 CaCl <sub>2</sub>	5.28 ± 0.03 abc	0.74 ± 0.12 abc	2.80 ± 0.29 ab	0.963
	25	0.01 CaCl <sub>2</sub>	5.54 ± 0.02 b	0.89 ± 0.09 abc	3.32 ± 0.22 ab	0.963
	35	0.01 CaCl <sub>2</sub>	5.60 ± 0.12 abc	0.85 ± 0.02 <sup>e</sup> bc	3.32 ± 0.06 <sup>d</sup> a	0.997
	25	0.01 RFS	5.35 ± 0.07 abc	1.13 ± 0.11 abc	3.86 ± 0.29 <sup>d</sup> ab	0.966
	25	0.05 RFS	5.29 ± 0.03 abc	0.78 ± 0.03 <sup>d,e</sup> c	2.92 ± 0.08 <sup>d</sup> b	0.994

<sup>a</sup>Letters indicate statistically significant differences between treatments. Values with the same letter are not significantly different, while those with different letters are statistically distinct ( $\alpha = 0.05$ ). <sup>b</sup>Abbreviations: oxyfluorfen (OXY), rice field salinity (RFS) with a molar ratio of 10:1:2:1 NaCl:CaCl<sub>2</sub>:MgSO<sub>4</sub>:Na<sub>2</sub>SO<sub>4</sub>. <sup>c</sup>Calculated from data obtained when initial concentration ( $C_i$ ) is 0.015  $\mu\text{g}\cdot\text{g}^{-1}$ . <sup>d</sup>Significant difference ( $P < 0.05$ ) between sorption and desorption Freundlich parameter. <sup>e</sup>Freundlich slope ( $N$ ) significantly different ( $P < 0.05$ ) from 1.

assemblage of the Davis soil was composed of smectite, vermiculite, kaolinite, illite, and an interlayered mineral species as indicated by the partial collapse to 10.1 Å following the KCl-550 heat treatment (Figure S2d).

**Soil Sorption.** Sorption Freundlich parameters and log( $K_{oc}$ ) by treatment are summarized in Table 2, while Freundlich isotherms (untransformed and log transformed) are available in the Supporting Information (Figures S3 and S4). The percentage of OXY sorbed ranged from 62.2 to 84.6% with an average ( $\pm$ SE) of  $71.3 \pm 0.8\%$ , which is within the ideal range ( $>50\%$ ) for characterizing sorption.<sup>22</sup> Sorption log( $K_{oc}$ ) ranged from 4.79 to 5.19, indicating a high affinity of oxyfluorfen for the soil and in general agreement with values reported previously in the literature (3.03–5.60).<sup>16,27–30</sup> With this affinity, OXY is classified as hardly mobile to immobile in soil and as a nonleacher, posing minimal risk of leaching to groundwater from rice field soils.<sup>31,32</sup> Biggs soil treatments yielded greater log( $K_{oc}$ ) than Davis soil except for 0.05 M RFS treatments. For CaCl<sub>2</sub> treatments, log( $K_{oc}$ ) also increased significantly with temperature for both soils ( $P = 0.00807$ ). This pattern is consistent with previous observations that sorption to rice field soil is enhanced with temperature and is indicative that the effects of temperature had a greater impact on the affinity of OXY for the soil than increases in its solubility.<sup>33,34</sup> It is possible that temperature increases may lead to release of water layers attached to soil surfaces, facilitating the liberation of adsorption sites previously occupied by water molecules.<sup>35</sup> Increased diffusion into the

SOM matrix and changes in SOM structure at higher temperatures may have also played a role.<sup>36,37</sup> No significant differences in log( $K_{oc}$ ) were found between RFS and CaCl<sub>2</sub> treatments or with increased rice field salinity.

Sorption isotherms were well described by the transformed Freundlich model ( $R^2$  0.971–0.998), with OXY displaying ideal C-curve isotherm behavior characteristic of hydrophobic organic chemicals (HOCs) for most treatments.<sup>13</sup> S-curve isotherms for OXY in soil have also been described in the literature.<sup>29,38,39</sup> The patterns observed in these studies may lack environmental relevance, however, due to limitations in design, including the use of only three initial concentrations and exceedance of the aqueous solubility of OXY (0.1  $\mu\text{g}\cdot\text{mL}^{-1}$ , 25 °C) for all initial concentrations.

The Freundlich degree of nonlinearity ( $N$ ) ranged from 0.87 to 1.08, indicating moderate to high sorption linearity. This range agrees with those identified in the literature, which spans from 0.77 to 1.08 in nonrice field soils.<sup>30,40,41</sup> The overall sorption behavior of OXY in rice field soil can be described as highly linear, with the majority of treatment groups (8 out of 10) possessing slopes statistically indistinguishable ( $\alpha = 0.05$ ) from  $N = 1$  (see Table 2). These results indicate that sorption of OXY to rice field soil is relatively concentration-independent and binding site heterogeneity is low under the conditions tested.<sup>13</sup> While treatment groups had little impact on sorption  $N$  in general, significant differences ( $\alpha = 0.05$ ) were observed when comparing the slopes between Biggs soil treatment at the highest incubation temperature (35 °C) in 0.01 CaCl<sub>2</sub> and rice

**Table 4. Hysteresis Indices for OXY Desorption from California Rice Field Soil at Specific Residual Solution Phase Concentrations ( $C_e$ )<sup>a</sup>**

soil	temperature (°C)	salinity (M) <sup>b</sup>	lower			middle			upper		
			$C_e$ ( $\mu\text{g}\cdot\text{mL}^{-1}$ )	hysteresis index <sup>c</sup>		$C_e$ ( $\mu\text{g}\cdot\text{mL}^{-1}$ )	hysteresis index <sup>c</sup>		$C_e$ ( $\mu\text{g}\cdot\text{mL}^{-1}$ )	hysteresis index <sup>c</sup>	
Davis	15	0.01 CaCl <sub>2</sub>	0.0026	1.17	(0.47–2.21)	0.005	1.04	(0.51–1.77)	0.0119	0.88	(0.26–1.79)
	25	0.01 CaCl <sub>2</sub>	0.0024	0.91	(0.30–1.83)	0.005	0.95	(0.44–1.64)	0.0104	0.99	(0.36–1.89)
	35	0.01 CaCl <sub>2</sub>	0.0017	0.80	(0.22–1.68)	0.005	0.61	(0.20–1.17)	0.0098	0.50	(0.00–1.25)
	25	0.01 RFS	0.0023	1.12	(0.43–2.16)	0.005	1.33	(0.70–2.19)	0.0074	1.44	(0.71–2.47)
	25	0.05 RFS	0.0025	0.79	(0.23–1.62)	0.005	0.73	(0.28–1.33)	0.0135	0.64	(0.10–1.44)
Biggs	15	0.01 CaCl <sub>2</sub>	0.0029	1.44	(0.65–2.61)	0.005	1.09	(0.53–1.86)	0.0175	0.47	(–0.05–1.27)
	25	0.01 CaCl <sub>2</sub>	0.0030	1.55	(0.79–2.65)	0.005	1.42	(0.76–2.33)	0.0099	1.26	(0.54–2.32)
	35	0.01 CaCl <sub>2</sub>	0.0018	1.12	(0.45–2.08)	0.005	1.07	(0.51–1.83)	0.0088	1.04	(0.39–2.00)
	25	0.01 RFS	0.0031	2.06	(1.09–3.47)	0.005	2.16	(1.25–3.45)	0.0074	2.25	(1.26–3.69)
	25	0.05 RFS	0.0031	1.69	(0.84–2.94)	0.005	1.4	(0.74–2.33)	0.0129	0.92	(0.31–1.81)

<sup>a</sup>Lower and upper  $C_e$  selected based on observed residual solution phase concentrations for both sorption and desorption isotherms. A middle  $C_e$  value of  $0.005 \mu\text{g}\cdot\text{mL}^{-1}$  was selected for cross-treatment comparison. <sup>b</sup>Abbreviations: oxyfluorfen (OXY), rice field salinity (RFS) with a molar ratio of 10:1:2:1 NaCl:CaCl<sub>2</sub>:MgSO<sub>4</sub>:Na<sub>2</sub>SO<sub>4</sub>. <sup>c</sup>Simultaneous (lower, upper) confidence bounds ( $\alpha = 0.05$ ) indicated by parentheses. Bounds that do not include zero (0) indicate significant sorption–desorption hysteresis.

field salinities (Table 2). For Biggs soils, a decrease in  $N$  with incubation temperature was observed, with  $N$  being statistically distinguishable ( $P < 0.0001$ ) from 1 at the highest temperature treatment (35 °C). According to the dual-mode sorption model, increased temperatures are associated with increased diffusion into SOM matrix, where the distribution of binding site energy has greater heterogeneity.<sup>37</sup> As  $N$  has been shown mathematically to be an index of site energy distribution, with smaller  $N$  values indicating broader energy distribution, enhanced diffusion into the SOM aided by increased incubation temperatures may explain the observed trend for the Biggs soils.<sup>42</sup> Increasing temperature is also hypothesized to increase linearity (higher  $N$ ) by disrupting micropore structures and decreasing binding site heterogeneity as SOM gradually transitions into a more expanded (rubbery) state.<sup>37</sup> This creates a dynamic relationship between temperature and  $N$ , where competing mechanisms offset each other, and the overall impact is dependent on the thermal response and properties of the SOM. Thus, multiple contributing factors may be involved across treatments, and attribution to any one mechanistic rationale is not feasible.

Sorption  $\log(K_F)$  ranged from 2.92 to 3.44. These values are greater than those reported in the literature for nonrice field soils (1.23–2.36), indicating the sorptive affinity of these rice field soils for OXY may be greater than other soils.<sup>30,40,43</sup> No statistical differences ( $\alpha = 0.05$ ) were found between any treatments for sorption  $\log(K_F)$ , and no trends with temperature were identified. These results suggest that the sorption affinity of OXY to the soils is similar under the array of soils and rice field conditions tested.

**Soil Desorption.** Desorption Freundlich parameters by treatment are summarized in Table 3. OXY was poorly desorbed from soils, with percent desorption ranging from 9.3 to 27.0% with an average ( $\pm$ SE) of  $15.5 \pm 0.5\%$ . In general, desorption of OXY from soils is reported to be highly hysteretic with very little desorption under both experimental and field studies.<sup>29,38,40</sup> In a field dissipation experiment in Indian subtropical soil, a similar desorption range was observed, ranging from 0.38 to 35.2% of the applied quantity.<sup>29</sup> As OXY exhibits both high sorption affinity and poor desorption potential, it will likely accumulate and persist in soil, rendering it less bioavailable to microbial degradation.<sup>1</sup>

Although dissolved concentrations are likely to be low, soil erosion and transport via runoff will likely transport bound OXY to other aquatic sites, where it may accumulate in the sediment.

Desorption  $\log(K_{oc})$  was higher than sorption  $\log(K_{oc})$  for each treatment group and ranged from 5.07 to 5.60. Desorption  $\log(K_{oc})$  for the Biggs soil was also greater than Davis soil for all treatments (Table 3). The observed increase in desorption  $K_{oc}$  and low percent desorption are consistent with desorption generally being an activated process, where a molecule must surpass a potential energy barrier greater than or equal to the free energy change ( $\Delta G$ ) for sorption to the soil surface in order to release back into aqueous solution.<sup>44</sup> Desorption  $\log(K_{oc})$  increased with temperature, and a significant increase ( $P = 0.00021$ ) was seen between the 15 and 35 °C CaCl<sub>2</sub> treatments in Davis soils. Other significant differences based on treatment interactions for desorption  $\log(K_{oc})$  are identified in Table 3.

Desorption isotherms were well described by the transformed Freundlich model ( $R^2$  0.963–0.998). Desorption  $N$  values were generally lower than those for sorption and ranged from 0.74 to 1.13. The only report located that characterized desorption nonlinearity used a distinct definition of desorption  $N$ ; this will be expanded upon in the hysteresis section.<sup>40</sup>

Desorption  $\log(K_F)$  ranged from 2.80 to 3.86. The majority of desorption isotherms display higher apparent sorption affinity, as indicated by  $\log(K_F)$ , in comparison to that of the corresponding sorption isotherms. These increases were statistically distinguishable ( $P < 0.05$ ) for four of the observed occurrences and are considered a hallmark of sorption hysteresis in soil.<sup>24</sup>

$\log(K_F)$  and  $N$  for both sorption and desorption decreased with increasing RFS for all treatments, while  $\log(K_{oc})$  decreased with increasing rice field salinity for the majority of treatments (Tables 2 and 3). The effects of salinity on soil sorption are complex, and a variety of competing mechanisms influence outcomes. Salting-out effects are commonly observed for HOCs.<sup>14,15,33</sup> On the other hand, competitive interaction between solutes for binding sites on soil surfaces can decrease sorption.<sup>45</sup> Aqueous salinity levels are also known to alter the conformation and size of humic substances as well as the expansion and collapsing of the interlayers of clay mineral

fractions of soils.<sup>46,47</sup> Cation concentration and valency further moderate the degree and types of interactions that occur.<sup>48</sup> One or more of these factors has the potential to influence sorption affinity as well as binding site availability and heterogeneity. These dynamic mechanisms make it difficult to predict outcomes across varying chemicals, soils, and saline conditions with certainty. Under the rice field salinity conditions tested, however, factors reducing sorption to soil surfaces generally appear stronger than those enhancing it. Interestingly, the consistent decrease in *N* indicates that increased saline conditions may alter the heterogeneity of sorption binding sites accessed. It has been shown that even a small deviation in *N* can underly large contributions from hole-filling mechanisms, which play a crucial role in isotherm nonlinearity and sorption irreversibility.<sup>37</sup> This implies that variations in rice field salinity could impact sorption mechanism and reversibility through salinity-induced changes to SOM structure.

**Hysteresis.** Calculated HI ranged from 0.47 to 2.25 and are presented in Table 4. A midrange  $C_e$  value of  $0.005 \mu\text{g}\cdot\text{mL}^{-1}$  was also identified within the observed sorption and desorption isotherm ranges shared between all treatments and was selected to calculate a middle HI value for comparison. Graphs of hysteresis indices across the full range calculable from sorption and desorption isotherm data for each treatment are available in the Supporting Information (Figure S5).

Of the 50 individual HI values calculated, 49 showed significant hysteresis ( $\text{HI} > 0$ ;  $\alpha = 0.05$ ). Although hysteresis was not significant at the upper  $C_e$  for Biggs soil incubated at  $15^\circ\text{C}$  with  $0.01 \text{ M CaCl}_2$ , it was significant at middle and lower  $C_e$  levels for that treatment, suggesting hysteretic processes predominate across all treatments and the majority of  $C_e$  conditions. Overall, hysteresis was greater in Biggs soils and observed to increase with decreasing residual solution phase concentration. This pattern of concentration-dependent hysteresis is consistent with the dual-mode model of sorption, which holds that the contribution of hole-filling mechanisms is greater at low concentrations.<sup>37</sup> Binding sites accessed through this mechanism are thought to account for hysteresis due to higher energy of binding and limited availability to sorbing molecules.<sup>49</sup> A decrease in HI with increasing RFS was also observed for both soils across all  $C_e$  (Figure S5), indicating that hysteresis is sensitive to ionic strength, and the degree of binding irreversibility may vary site-to-site based on individual rice field salinity conditions. Possible mechanisms that could explain this observation include competitive sorption with ions for high energy binding sites or changes in SOM structure at high salinity that limit diffusion into or within the SOM matrix.<sup>49</sup>

Few Freundlich isotherm studies are available in the literature for OXY, and only a single study was located that characterized the degree of desorption nonlinearity and hysteresis in soil. In a batch equilibrium study in two Spanish soils, desorption of OXY was found to be highly hysteretic in both soils through calculation of another index used to characterize hysteresis known as the thermodynamic index of irreversibility (TII).<sup>40</sup> TII represents the difference in measured desorption state versus a hypothetically fully reversible state, with indices of 0 representing complete reversibility and trending toward 1 with complete irreversibility.<sup>50</sup> Methodology for calculation of TII are presented in the Supporting Information. TII calculated in the two Spanish

soils ranged from 0.927 to 0.975 in sandy clay loam and silty clay loam, respectively, indicating a high irreversibility of binding.

For comparison, TII was also calculated using the data produced in this investigation and are presented in the Supporting Information (Tables S2 and S3). Calculated TII ranged from 0.128 to 0.915, indicating that binding of OXY to soil was mostly reversible to highly irreversible. However, the majority (86%) of the TII calculated were  $\geq 0.75$ , with an average value of 0.80, suggesting that sorption to the soil is predominantly a highly irreversible process.<sup>50</sup> Calculated TII were also generally greater in treatments with Biggs soil and exhibited inverse concentration-dependency in a manner similar to HI. Overall, results for both indices agree and indicate the occurrence of pronounced sorption–desorption hysteresis under California rice field conditions.

Hysteretic processes can profoundly impact the overall fate of herbicides in the environment. Herbicides irreversibly bound to the soil are typically not bioavailable for microbial degradation, leading to persistence.<sup>49</sup> Resistance to entering the water column may further inhibit environmental half-lives as photolysis is the primary route of degradation for OXY.<sup>6</sup> Aging within the soil may result in further sequestration over time, although this diffusion-limited process may be impeded somewhat due to the high sorption affinity of OXY for soil.<sup>37</sup> While sorption results in this study suggest that OXY will be found predominantly in rice field sediment, this extended aging profile may create longer periods where the labile fractions of OXY residues may be mobilized into overlying field water, especially when water turnover and dissolved/suspended organic matter levels are high. Once in the water column, OXY may be subject to transport off-field via runoff and erosion.

Accurate determination of herbicide mass balance in sediment and surface waters over time is paramount to predicting fundamental interests, such as effective water holding periods and risk to nontarget organisms, particularly aquatic species highly susceptible to OXY toxicity. Factors modulating the partitioning behavior for OXY, such as rice field salinity and soil characteristics, must also be considered. Significant hysteresis is also anticipated in rice field soil, and models that fail to incorporate this nonideal behavior are likely to provide estimates that differ markedly from reality. Thus, careful consideration of these principal factors will provide the foundation for making safe and effective decisions regarding the use of OXY as an herbicide in California rice fields.

## ■ ASSOCIATED CONTENT

### SI Supporting Information

The Supporting Information is available free of charge at <https://pubs.acs.org/doi/10.1021/acsagscitech.3c00341>.

Methods and figures for FTIR and XRD analysis; mass spectrometer acquisition parameters; Freundlich isotherms; and hysteresis calculations (PDF)

## ■ AUTHOR INFORMATION

### Corresponding Author

David J. Bonnar – Department of Environmental Toxicology, University of California, Davis, California 95616, United States; [orcid.org/0000-0002-9736-215X](https://orcid.org/0000-0002-9736-215X); Phone: (530) 752-2534; Email: [djbonnar@ucdavis.edu](mailto:djbonnar@ucdavis.edu)

## Authors

Jeff P. Eichler – Department of Environmental Toxicology, University of California, Davis, California 95616, United States

Sanjai J. Parikh – Department of Land, Air and Water Resources, College of Agricultural and Environmental Sciences, University of California, Davis, California 95616, United States

Andrew Blandino – Department of Statistics, College of Letters and Science, University of California, Davis, California 95616, United States

Rebecca A. Lybrand – Department of Land, Air and Water Resources, College of Agricultural and Environmental Sciences, University of California, Davis, California 95616, United States; [orcid.org/0000-0001-7811-9093](https://orcid.org/0000-0001-7811-9093)

Madison L. Morris – Department of Land, Air and Water Resources, College of Agricultural and Environmental Sciences, University of California, Davis, California 95616, United States

Matt J. Hengel – Department of Environmental Toxicology, University of California, Davis, California 95616, United States

Ronald S. Tjeerdema – Department of Environmental Toxicology, University of California, Davis, California 95616, United States

Complete contact information is available at:

<https://pubs.acs.org/10.1021/acsagscitech.3c00341>

## Funding

This work was funded by the Donald G. Crosby Endowment in Environmental Chemistry.

## Notes

The authors declare no competing financial interest.

## ACKNOWLEDGMENTS

The authors thank Z. Redman, K. Al-Khatib, and A. Beccera-Alvarez for their assistance.

## ABBREVIATIONS USED

OXY, oxyfluorfen;  $K_F$ , Freundlich constant;  $N$ , Freundlich exponent;  $HI$ , hysteresis index;  $K_d$ , soil-water partition coefficient;  $K_{oc}$ , organic carbon-water partition coefficient; CA, California; HPLC, high-pressure liquid chromatography;  $f_{om}$ , fraction organic matter;  $f_{oc}$ , fraction organic carbon; CEC, cation exchange capacity; UC, University of California; U.S., United States; SOM, soil organic matter; OM, organic matter; FTIR, Fourier transform infrared; XRD, X-ray diffraction; OECD, Organisation for Economic Co-operation and Development; RFS, rice field salinity; d5-OXY, d5-oxyfluorfen; PTFE, polytetrafluoroethylene; SE, standard error;  $n$ , sample size; LC-MS/MS, liquid chromatography-tandem mass spectrometry; QQQ, triple quadrupole mass spectrometer; MDL, method detection limit;  $ML$ , method quantitation limit;  $q_s^s$ , soil concentration of OXY at sorption equilibrium;  $m_{aq}$ , mass of aqueous phase;  $C_i$ , initial aqueous phase concentration of OXY;  $C_{aq}^s$ , aqueous phase concentration of OXY at sorption equilibrium;  $m_s$ , mass of soil;  $q_s^d$ , soil concentration of OXY at desorption equilibrium;  $m_{aq}^i$ , initial aqueous phase mass;  $m_{aq}^{dec}$ , mass of aqueous phase decanted;  $m_{aq}^r$ , mass of aqueous phase after replacing decanted liquid;  $C_{aq}^d$ , aqueous phase concentration of OXY at desorption equilibrium;  $q_s$ , soil concentration of OXY at equilibrium;  $C_{aq}$ , water concentration of oxy

at equilibrium;  $C_e$ , residual solution phase concentration;  $q_e^d$ , solid-phase concentration at desorption equilibrium at a given  $C_e$ ;  $q_e^s$ , solid-phase concentration at sorption equilibrium at a given  $C_e$ ; nlme, nonlinear mixed-effects; gls, generalized least-squares; IR, infrared; C = O, carbonyl; HOC, hydrophobic organic chemical;  $\Delta G$ , free energy change; TII, thermodynamic index of irreversibility

## REFERENCES

- (1) U.S. Environmental Protection Agency (USEPA). *Reregistration Eligibility Decision (RED) for Oxyfluorfen* Office of Prevention, Pesticides, and Toxic Substances: Washington, D.C.; 2002.
- (2) U.S. Environmental Protection Agency (USEPA). *Oxyfluorfen Proposed Interim Registration Review Decision* Office of Pesticide Programs: Washington, D.C.; 2021.
- (3) California Cooperative Rice Research Foundation (CCRRF). *The Rice Experiment Station 2017 Report USA Rice Outlook Conference*: San Antonio, TX; 2017.
- (4) Galvin, L. B.; Becerra-Alvarez, A.; Al-Khatib, K. Assessment of Oxyfluorfen-Tolerant Rice Systems and Implications for Rice-Weed Management in California. *Pest Manage. Sci.* **2022**, *78* (11), 4905–4912.
- (5) U.S. Environmental Protection Agency (USEPA). *Revised Environmental Fate and Effects Division Preliminary Risk Assessment for the Oxyfluorfen Registration Eligibility Decision Document* Office of Prevention, Pesticides, and Toxic Substances: Washington, D.C.; 2001.
- (6) California Department of Pesticide Regulation (DPR). *Environmental Fate and Toxicology of Oxyfluorfen* Sacramento: CA; 2017.
- (7) United States Department of Agriculture (USDA) Rice Sector at a Glance. <https://www.ers.usda.gov/topics/crops/rice/rice-sector-at-a-glance/> (accessed January 14, 2023).
- (8) Board, J. E.; Peterson, M. L.; Ng, E. Floret Sterility in Rice in a Cool Environment. *Agron. J.* **1980**, *72*, 483–487.
- (9) Roel, A.; Mutters, R. G.; Eckert, J. W.; Plant, R. E. Effect of Low Water Temperature on Rice Yield in California. *Agron. J.* **2005**, *97* (3), 943–948.
- (10) Marcos, M.; Sharifi, H.; Grattan, S. R.; Linqvist, B. A. Spatio-Temporal Salinity Dynamics and Yield Response of Rice in Water-Seeded Rice Fields. *Agric. Water Manage.* **2018**, *195*, 37–46.
- (11) Grattan, S. R.; Zeng, L.; Shannon, M. C.; Roberts, S. R. Rice Is More Sensitive to Salinity Than Previously Thought. *Calif. Agric.* **2002**, *56*, 189–198.
- (12) Lindquist, B.; Al-Khatib, K.; Swett, C.; Espino, L.; Leinfelder-Miles, M.; Brim-DeForest, W.; Mckenzie, K. *Weed Management: Cultural Methods, in Rice Production Manual*; University of California, Agriculture and Natural Resources (UC/ANR): Davis, CA, 2018.
- (13) Essington, M. E. *Soil and Water Chemistry: An Integrative Approach*; CRC Press, 2004.
- (14) Means, J. C. Influence of Salinity Upon Sediment-Water Partitioning of Aromatic-Hydrocarbons. *Mar. Chem.* **1995**, *51* (1), 3–16.
- (15) Tremblay, L.; Kohl, S. D.; Rice, J. A.; Gagne, J. P. Effects of Temperature, Salinity, and Dissolved Humic Substances on the Sorption of Polycyclic Aromatic Hydrocarbons to Estuarine Particles. *Mar. Chem.* **2005**, *96* (1–2), 21–34.
- (16) Shaner, D. L. *Herbicide Handbook*, 10th ed.; Weed Science Society of America: Lawrence, 2014; p 513.
- (17) Sondhia, S. Persistence of Oxyfluorfen in Soil and Detection of Its Residues in Rice Crop. *Toxicol. Environ. Chem.* **2009**, *91* (3), 425–433.
- (18) United States Department of Agriculture, Natural Resources Conservation Service Web Soil Survey. <https://websoilsurvey.sc.egov.usda.gov/> (accessed October 29, 2020).
- (19) Soil Survey Staff, Natural Resources Conservation Service, United States Department of Agriculture Official Series Descriptions (OSD). <https://www.nrcs.usda.gov/resources/data-and-reports/official-soil-series-descriptions-osd> (accessed September 6, 2021).

- (20) University of California Davis. Analytical Laboratory, College of Agriculture and Environmental Sciences. <http://anlab.ucdavis.edu> (accessed September 27, 2021).
- (21) US Salinity Laboratory Staff. Ph Reading of Saturated Soil Paste. P. 102. In *Diagnosis and Improvement of Saline and Alkali Soils. Usda Agricultural Handbook 60*; Richards, L. A., Ed.; U.S. Government Printing Office: Washington, DC, 1954.
- (22) OECD. *Test No. 106: Adsorption – Desorption Using a Batch Equilibrium Method*, Guideline for the Testing of Chemicals; Organisation for Economic Co-operation and Development: Paris, France; 2000.
- (23) Huang, W. L.; Yu, H.; Weber, W. J. Hysteresis in the Sorption and Desorption of Hydrophobic Organic Contaminants by Soils and Sediments - 1. A Comparative Analysis of Experimental Protocols. *J. Contam. Hydrol.* **1998**, *31* (1–2), 129–148.
- (24) Weber, W. J.; Huang, W. L.; Yu, H. Hysteresis in the Sorption and Desorption of Hydrophobic Organic Contaminants by Soils and Sediments - 2. Effects of Soil Organic Matter Heterogeneity. *J. Contam. Hydrol.* **1998**, *31* (1–2), 149–165.
- (25) R Core Team. *A Language and Environment for Statistical Computing*, <https://www.R-project.org/>.
- (26) Pinheiro, J.; Bates, D.; R Core, Team. *Nlme: Linear and Nonlinear Mixed Effects Models*, R package version 3.1–162; R Foundation for Statistical Computing: Vienna, Austria, 2023.
- (27) Alister, C. A.; Gomez, P. A.; Rojas, S.; Kogan, M. Pendimethalin and Oxyfluorfen Degradation under Two Irrigation Conditions over Four Years Application. *J. Environ. Sci. Health, Part B* **2009**, *44* (4), 337–343.
- (28) Calderon, M. J.; De Luna, E.; Gomez, J. A.; Hermosin, M. C. Herbicide Monitoring in Soil, Runoff Waters and Sediments in an Olive Orchard. *Sci. Total Environ.* **2016**, *569–57*, 416–422.
- (29) Janaki, P.; Sathya Priya, R.; Chinnusamy, C. Field Dissipation of Oxyfluorfen in Onion and Its Dynamics in Soil under Indian Tropical Conditions. *J. Environ. Sci. Health, Part B* **2013**, *48* (11), 941–947.
- (30) Wu, C.; Liu, X. G.; Wu, X. H.; Dong, F. S.; Xu, J.; Zheng, Y. Q. Sorption, Degradation and Bioavailability of Oxyfluorfen in Biochar-Amended Soils. *Sci. Total Environ.* **2019**, *658*, 87–94.
- (31) *Fao Pesticide Disposal Series 8. 486 Assessing Soil Contamination. A Reference Manual*. Rome; Italy: 2000.
- (32) Gustafson, D. I. Groundwater Ubiquity Score: A Simple Method for Assessing Pesticide Leachability. *Environ. Toxicol. Chem.* **1989**, *8*, 339–357.
- (33) Redman, Z. C.; Tjeerdema, R. S. Impact of Simulated California Rice-Growing Conditions on Chlorantraniliprole Partitioning. *J. Agric. Food Chem.* **2018**, *66* (8), 1765–1772.
- (34) Williams, K. L.; Gladfelder, J. J.; Quigley, L. L.; Ball, D. B.; Tjeerdema, R. S. Dissipation of the Herbicide Benzobicyclon Hydrolyzate in a Model California Rice Field Soil. *J. Agric. Food Chem.* **2017**, *65* (42), 9200–9207.
- (35) Moreale, A.; Bladel, R. V. Soil Interactions of Herbicide-Derived Aniline Residues: A Thermodynamic Approach. *Soil Sci.* **1979**, *127* (1), 1–9.
- (36) Lu, Y.; Pignatello, J. J. Demonstration of the "Conditioning Effect" in Soil Organic Matter in Support of a Pore Deformation Mechanism for Sorption Hysteresis. *Environ. Sci. Technol.* **2002**, *36* (21), 4553–4561.
- (37) Xing, B. S.; Pignatello, J. J. Dual-Mode Sorption of Low-Polarity Compounds in Glassy Poly(Vinyl Chloride) and Soil Organic Matter. *Environ. Sci. Technol.* **1997**, *31* (3), 792–799.
- (38) Fadayomi, O.; Warren, G. F. Adsorption, Desorption, and Leaching of Nitrofen and Oxyfluorfen. *Weed Sci.* **1977**, *25* (2), 97–100.
- (39) Sireesha, A.; Rao, P. C.; Rao, P. V.; Ramalakshmi, C. S.; Swapna, G. Adsorption Desorption of Pendimethalin and Oxyfluorfen in Soils of Andhra Pradesh. *J. Res. ANGRAU* **2013**, *41*, 1–10.
- (40) Calderón, M. J.; Real, M.; Cabrera, A.; Koskinen, W. C.; Cornejo, J.; Hermosin, M. C. Influence of Olive Oil Mill Waste Amendment on Fate of Oxyfluorfen in Southern Spain Soils. *Clean-Soil Air Water* **2015**, *43* (7), 1107–1113.
- (41) Lewis, K. A.; Tzilivakis, J.; Warner, D. J.; Green, A. An International Database for Pesticide Risk Assessments and Management. *Hum. Ecol. Risk Assess.: Int. J.* **2016**, *22* (4), 1050–1064.
- (42) Carter, M. C.; Kilduff, J. E.; Weber, W. J. Site Energy Distribution Analysis of Preloaded Adsorbents. *Environ. Sci. Technol.* **1995**, *29* (7), 1773–1780.
- (43) U.S. Environmental Protection Agency (USEPA). *Environmental Fate and Ground Water Branch Review Action for Oxyfluorfen* Environmental Fate and Effects Division: Washington, D.C.; 1993.
- (44) Sawhney, B. L.; Brown, K. W. *Reactions and Movement of Organic Chemicals in Soils*; Soil Science Society of America, Inc., American Society of Agronomy, Inc.: Madison, WI, 1989.
- (45) Xing, B. S.; Pignatello, J. J.; Gigliotti, B. Competitive Sorption between Atrazine and Other Organic Compounds in Soils and Model Sorbents. *Environ. Sci. Technol.* **1996**, *30* (8), 2432–2440.
- (46) Baalousha, M.; Motelica-Heino, M.; Le Coustumer, P. Conformation and Size of Humic Substances: Effects of Major Cation Concentration and Type, Ph, Salinity, and Residence Time. *Colloids Surf., A* **2006**, *272* (1–2), 48–55.
- (47) Shainberg, I.; Letey, J. Response of Soils to Sodic and Saline Conditions. *Hilgardia* **1984**, *52* (2), 1–57.
- (48) Cai, W. W.; Navarro, D. A.; Du, J.; Ying, G. G.; Yang, B.; McLaughlin, M. J.; Kookana, R. S. Increasing Ionic Strength and Valency of Cations Enhance Sorption through Hydrophobic Interactions of Pfas with Soil Surfaces. *Sci. Total Environ.* **2022**, *817*, No. 152975, DOI: 10.1016/j.scitotenv.2022.152975.
- (49) Pignatello, J. J.; Xing, B. S. Mechanisms of Slow Sorption of Organic Chemicals to Natural Particles. *Environ. Sci. Technol.* **1996**, *30* (1), 1–11.
- (50) Sander, M.; Lu, Y.; Pignatello, J. J. A Thermodynamically Based Method to Quantify True Sorption Hysteresis. *J. Environ. Qual.* **2005**, *34* (3), 1063–1072.